

A new approach to contrast enhancement in MAGICA gel dosimeter image with MRI technique

S.M. Abtahi¹, M. Shahriari^{1*}, M.H. Zahmatkesh², H. Khalafi³,
Sh. Akhlaghpour², S. Bagheri²

¹Shahid Beheshti University, Nuclear Engineering Faculty, Tehran, Iran

²Novin Medical Radiation Institute, Tehran, Iran

³Nuclear Science and Technology Research Institute, Tehran, Iran

Background: Sensitivity and resolution are two main parameters that have to be measured in gel dosimetry. However, the resolution in gel is strongly dependant on gel composition. Selection of optimum method in dose response readout and proper values of parameters can result in noise reduction as well as improvement of contrast, and spatial resolution considerably. **Materials and Methods:** MAGICA polymer gel dosimeters were manufactured and irradiated to different doses using a ⁶⁰Co therapy unit. Imaging was performed in a 0.5T MRI with 8 echoes in air and water as a hydrogenous environment. Imaging condition was kept constant, as much as possible, in both imaging modalities. **Results:** Images obtained from these two procedures were compared quantitatively. R2- dose curves have three different sections, sensitivity obtained in these three sections were 1.039, 1.671, 1.260 Gy⁻¹S⁻¹ and 1.032, 1.729, 1.37 Gy⁻¹S⁻¹ for water and air respectively. Calibration errors were investigated and graphically were compared in two different methods. **Conclusion:** Imaging in water medium for doses lower than 17 Gy led to a small reduction in spatial resolution was exchanged to a considerable increase of contrast in R2 map. For doses higher than 17 Gy, imaging in water or air was preferred depending on the importance of contrast or spatial resolution. **Iran. J. Radiat. Res., 2008; 6 (3): 151-156**

Keywords: Gel dosimeter, MAGICA, resolution, MRI, R2 map.

INTRODUCTION

Gel dosimetry has been examined as a clinical dosimeter since the 1950s. During the last two decades, however, the number of investigators in this field has increased rapidly, and the body of knowledge regarding gel dosimetry has expanded considerably. Gel dosimetry is still in it's a

research phase, and the introduction of this tool into clinical use is proceeding slowly⁽¹⁾. In this study a new type of gel dosimeter with acronym of MAGICA was used. This type of gel dosimeter was manufactured by adding agarose to the ingredient of MAGIC gel dosimeter⁽²⁾. MAGICA gel dosimeter was manufactured in Novin Radiation Medicine Institute (I.R. Iran) in 2004⁽³⁾.

Two major advantages of polymer gel dosimeters were their ability to determine integrated 3D dose distribution, as well as their ability to form in different shapes⁽⁴⁾. In fact, polymer gel dosimeters were monomers which distributed in a gelling matrix. Ionizing radiations convert these monomers to polymers via distinguished mechanism⁽⁵⁾. The polymerization degree is dependant on the absorbed dose in gel dosimeter. After polymerization, magnetic properties of polymer surrounding protons are changed⁽⁴⁾. These changes could be exhibited by magnetic resonance imaging. The spin-spin relaxation rate $R2=1/T2$ is related to the absorbed dose which was delivered to a gel phantom. Artifacts have always been major problems in medical imaging, and gel dosimeter MR images are not immune from these problems⁽⁶⁻⁸⁾.

A major problem in MRI read out method, especially when dealing with small

*Corresponding author:

Dr. Majid Shahriari, Nuclear Engineering Faculty,
University of Shahid Beheshti, P. O. Box 19839-
63113, Tehran, Iran

Fax: +98 21 22431780

E-mail: m-shahriari@sbu.ac.ir

vials (or other gel container) is the serious reduction of contrast in edges. Since in gel dosimetry spatial resolution has a great importance, one should be careful in using image processing filters. In this study contrast enhancement of MAGICA gel dosimeters with MRI in water environment and noise in the dose map was investigated. Contrast and noise of R2 (=1/T2) in gel MRI images in water and air were also compared and optimum condition for MAGICA gel dosimeters MR imaging was obtained for the best contrast and resolution.

MATERIALS AND METHODS

The composition of MAGICA gel dosimeter is given in table 1. For fabrication of MAGICA gel dosimeter, gelatin (Type A, 300 Bloom, Sigma-Aldrich Co, USA) was added to 65% of de-ionized water (BDH Laboratory Supplies, UK) and allowed to swell for half an hour in room temperature. An electrical heating plate provided with magnetic stringing, was used to heat the solution up to 50 °C. Another heating and stirring plate was used to prepare the agarose (Sigma-Aldrich Co, USA) solution. When the gelatin and agarose solution reached to the same temperature (45 °C) the two solutions were mixed and allowed to cool down to a gelling agent of 37°C. Then the mixture of hydroquinone (BDH Laboratory Supplies, UK), methacrylic acid (Merck, Germany), CuSO₄ (BDH Laboratory Supplies, UK) and ascorbic acid (BDH Laboratory Supplies, UK) was added to the mixture of agarose and gelatin.

When the preparation of final polymer gel solution was completed, it was transferred into test tubes and phantoms, allowed to set in a refrigerator at about 4°C. Agarose and gelatin provided a gelling matrix and kept the monomers and polymers in 3D. Addition of agarose increased

Table1. Composition of 1000 g MAGICA gel dosimeter.

Component	Amount (g)
Gelatin	80
Agarose	5
Methacrylic acid	90
Ascorbic acid	0.352
CuSO ₄ ·5H ₂ O	0.015
Hydroquinone	2
Ultra-pure water (HPLC grade)	823

the strength of the gel and kept 3D distribution of dose after irradiation.

Some free radicals are always found in water that can initiate the polymerization reaction (self polymerization). Hydroquinone was used to band these free radicals and to inhibit self polymerization. Under irradiation H and OH radicals were produced and initiated the polymerization reaction.

Methacrylic acid was a monomer that converts to polymer by irradiation. Ascorbic acid acted as antioxidant that scavenged the oxygen of the gel and acted as polymerization inhibitor. CuSO₄ was a catalyst for binding the oxygen to ascorbic acid (2, 9, 10).

Irradiation

Gels were irradiated with a clinical ⁶⁰Co system (Teratron II 780C, Canada). To create scattered radiation, the same as human body, the gels were put under 5Cm water during irradiation. The radiation field is 20 × 20 cm² and dose rate was 80 cGy/min. Dosimetry of gamma source was done by ionization chamber (Farmer, Nuclear Enterprise Co., U.K.).

Imaging and preparing an R2 map

There are several methods for dose response readout in gel dosimetry (1, 11). In this study the proton magnetic properties variation was exhibited by magnetic

resonance imaging (MRI). Gels were imaged using a 0.5T MRI system (Philips). An MRI protocol that minimized the noise in 0.5T MR image was found (table 2).

Table 2. Optimum imaging protocol used in a Philips 0.5T MRI systems; TE: echo time, TR: repetition time, ES: space between echoes, Echo No.: number of echoes, NEX: Number of averages, FOV: Field of view and, No. Slice: number of slices.

TE (ms)	20
TR (ms)	1500
ES (ms)	20
Echo No.	8
NEX	3
FOV (mm)	256 × 256
Slice thickness (mm)	3
No. slice	1

Container was centered in the head coil. The gel phantom which was put in head coil had a higher signal to noise ratio in comparison with body coil. To ensure that the obtained R2 values were not influenced by possible temperature gradients in the gel, phantoms were left in MRI room 24 h before scanning.

Since the gel temperature during imaging increased up to 3 °C, a little motion artifact would exist in MR image (8). 24 hours after irradiation, it was sure that the polymerization mechanism was completed. R2 (=1/T2) maps were computed using modified radiotherapy gel dosimetry image processing software coded in MATLAB.

Dose error calculation and minimum detectable dose

There are three methods for R2 map extraction from MR Images: a) two points method, b) many point method, and c) Maximum-likelihood estimation (12).

In many points method the R2 map is obtained by fitting the MRI signals in different echoes in equation (1).

$$S = S_0 \exp(-R_2 TE) \quad (1)$$

Where S_0 is the signal corresponding with the unrelaxed magnetization or, from a theoretical point of view, which corresponds with an echo time TE=0.

To obtain dose from R2 map, calibration curve was needed. Gel dose response vs. absorbed dose was linear in the different ranges and follows the equation (2).

$$R_{2i} = R_{2,0} + \alpha D_i \quad (2)$$

The R_{2i} value in each test tube i is defined as the mean R2 in a region of interest (ROI) of uniform dose. The standard deviation of the R2 values in an ROI is also determined. This value is called σ_{call} . If N_{ROI} is the number of pixels in ROI then the standard errors of the R2 mean value is given by:

$$\frac{\sigma_{call}}{\sqrt{N_{ROI}}}$$

The standard errors had little differences and the mean value of standard error was used. The calibration dose error will be (12)

$$\sigma_{D^*} = \frac{\sigma_{call}}{\alpha \sqrt{N_{ROI}}} \sqrt{\frac{(D^* - \bar{D})^2}{\sum_1^{N_{ROI}} (D_i - \bar{D})^2} + \frac{1}{N_{call}}} \quad (3)$$

In which D^* , \bar{D} and N_{call} are predicted dose from an unknown R2, mean calibration dose and number of calibration points respectively.

D_{Δ^p} is defined as the minimal separation between two absorbed dose such that they may be distinguished with a given level of confidence (p). The minimal detectable dose (MDD) is D_{Δ^p} as the dose approach to zero. D_{Δ^p} can be written as:

$$D_{\Delta^p}^p = k_p \sqrt{2} \sigma_D \quad (4)$$

Where k_p is the coverage factor that is given in ISO (International Organization for Standardization) 1995 (13) (table 3).

Table 3. Coverage factor adapted from ISO1995.

Level of confidence	K_p
95%	1.96
68%	1
52%	$1/\sqrt{2}$

RESULTS

Since the experiments were performed in water environment, the effect of contrast enhancement in MAGICA gel dosimeter with MRI technique was investigated to achieve good results. MR images in water and air were obtained while all other conditions of imaging were the same, e.g. in both case containers fixed in the head coil and left for few minutes to avoid motion artifact due to water disturbance in the container. Figures 1 and 2 illustrate the R2 maps from imaging in air and water

respectively.

As it can be seen in figure 1 and 2, imaging in water environment increased the contrast noticeably. When small phantom was used this contrast enhancement for real boundary of R2 map determination was very important.

R2 map in each image was calculated with the selection of regions of interest (ROI) with equal number of pixels and the mean values of R2 and standard deviation of R2 in those regions were calculated. In this study the number of pixels was 364 and the ROIS were selected in the center of the phantoms. Figures 3 and 4 illustrate the change of $R2 = [1/T2]$ as a function of absorbed dose by imaging in air and water. Standard deviations in both figures are also shown. Investigation of these two curves shows that each of these curves can be segmented into 3 linear part: a), 1-8Gy; b), 8-17Gy; c), 17-22 Gy.

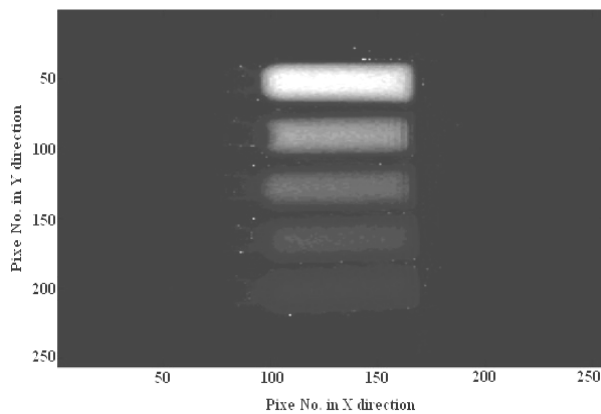


Figure 1. R2 map from imaging in air.

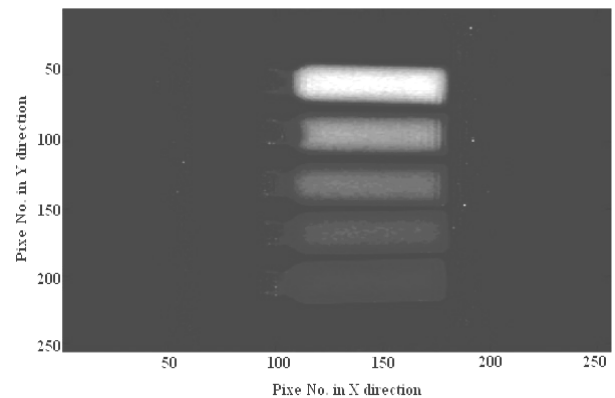


Figure 2. R2 map from imaging in water; imaging in water environment has increased the contrast noticeably.

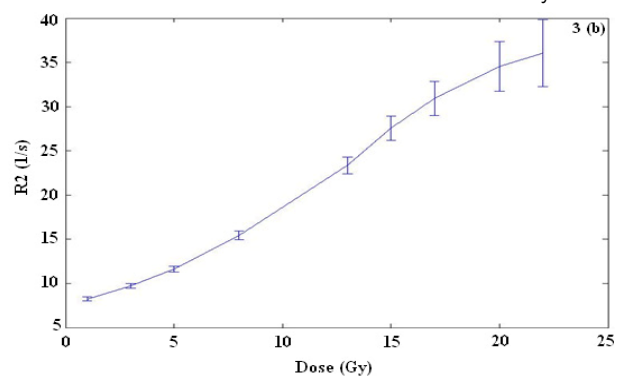
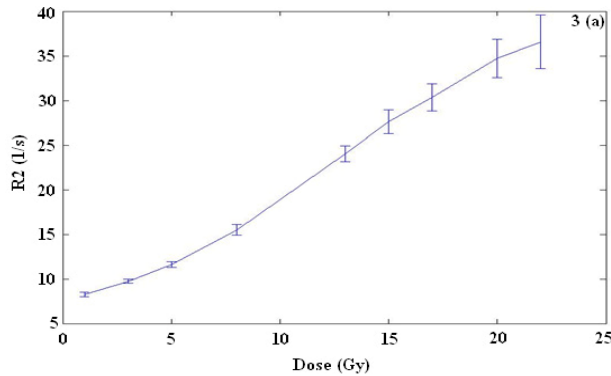


Figure 3. The change of $R2=[1/T2]$ as a function of absorbed dose for MAGICA gel dosimeter by imaging in air (a) and water (b). Error bars show standard deviation of mean values.

Mean value of the slopes of dose response curves in two methods of imaging is given in table 4..

Table 4. The slope compression for two methods of imaging.

Dose range	The slope for imaging in water	The slope for imaging in air
1-8 Gy	1.039	1.032
8-17 Gy	1.671	1.729
17-22 Gy	1.260	1.037

Figure 4 illustrates the values of calibration dose error (D^*) in two images for different dose ranges.

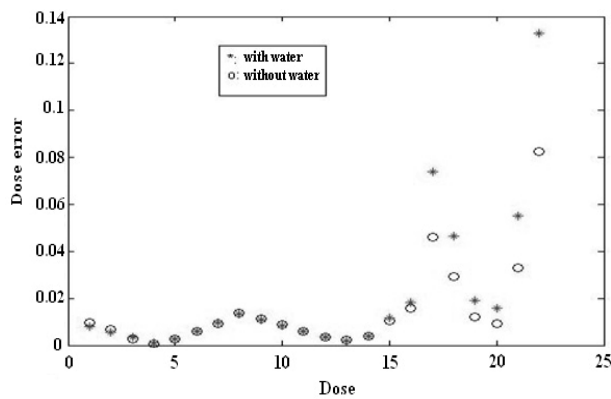


Figure 4. Comparison of calibration errors for two imaging methods.

DISCUSSION

As shown in figures 1 and 2, by imaging in water environment, R2 map contrast has enhanced noticeably. The contrast enhancement could be referred to susceptibility artifact removing. Susceptible artifact occurred as the result of microscopic gradients or variation in the magnetic field strength that occurred near the interface of substance of different magnetic susceptibility. This gradient caused dephasing at the interface and signal loss⁽¹⁴⁾. Since magnetic property of gel was very similar to water, the artifact was reduced and the contrast enhanced noticeably when imaging was performed in water environment.

As it can be seen in figure 4, calibration dose error values were similar up to 17

Gy, but for the dose range of 17-22 Gy imaging in water environment, the error increased noticeably. Dose error increased with increasing calibration error⁽¹²⁾, and as it can be seen from equations 3 and 4, increasing in dose error increases D_{Δ}^p , and spatial dose resolution had decreased. However, object related geometrical distortions may be compensated with the first measuring, or simulating the local magnetic field distortions caused by susceptibility differences and chemical shift artifacts. These magnetic field maps can then be used to construct a correction template that can be used to correct the parametric images. Another method to correct for local magnetic field distortions is by view angle-tilting. The advantage of this method was having no post-processing. The disadvantage of the method, however, is the broadened point-spread function. It should be emphasized that the artifacts act on a pixel-related scale instead of a geometrical scale. Increasing the resolution decreased the artifact on a geometrical scale. Another important parameter was the receiver bandwidth. The distortions were inversely proportional to the receiver bandwidth. However, increasing the bandwidth decreased the signal-to-noise ratio⁽¹⁵⁾. All of these methods were complicated and time consuming, but using of water environment for MR imaging was simple and effective for phantom shape preservation.

In small sample of gel dosimeters, determination of dose boundary has a great importance imaging in water medium. As it can be seen in figure 5, imaging in water medium with high rang doses resulted in a high value of error which results in increase of minimal detectable dose difference within a given level of confidence, p (D_{Δ}^p) and this has caused the reduction of dose spatial resolution. The reduction of spatial resolution in doses lower than 17 Gy was not considerable; therefore, with imaging in water medium, a small reduction in spatial resolution was exchanged to considerable increase

of contrast in R2 map which was important. In doses higher than 17 Gy, significance of contrast and spatial resolution imaging in water was preferable.

ACKNOWLEDGEMENT

This research is supported by the Novin Medical Radiation Institute (Tehran, I.R. Iran). Useful discussions with Mr. A Rahimi is highly appreciated. The authors also are thankful to Mrs. A. Madahian and Mr. H. Shahabian for their kind efforts in imaging process.

REFERENCES

1. Ibbott GS (2004) Application of gel dosimetry. *Journal of Physics*, **3**: 58-77.
2. Fong PM, Keil DC, Does MD, Gore JC (2001) Polymer gels for magnetic resonance imaging of radiation dose distributions at normal room atmosphere. *Physics in Medicine and Biology*, **46**: 3105-3113.
3. Zahmatkesh MH, Kousari R, Akhlaghpour S, Bagheri SA (2004) MRI gel dosimetry with methacrylic acid, ascorbic acid, hydroquinon and copper in agarose (MAGICA) gel. In: Preliminary Proceedings of DOSGEL 2004; Ghent, Belgium
4. De Deene Y (2004) Essential characteristics of polymer gel dosimeters. *Journal of Physics*, **3**: 34-57.
5. De Deene Y, Hurley C, Venning A, Vergote K, Mather M, Healy BJ, et al. (2002) A basic study of some normoxic polymer gel dosimeters. *Physics in Medicine and Biology*, **47**: 3441-3463.
6. Deene YD, Wagter CD, Neve WD, Achten E (2000) Artefacts in multi-echo T₂ imaging for high-precision gel dosimetry: I. Analysis and compensation of eddy currents. *Physics in Medicine and Biology*, **45**:1807-1823.
7. De Deene Y, Wagter CD, Neve WD, Achten E (2000) Artefacts in multi-echo T₂ imaging for high-precision gel dosimetry: II. Analysis of B1-field inhomogeneity. *Physics in Medicine and Biology*, **45**:1825-1839.
8. Deene YD and Wagter CD (2001) Artefacts in multi-echo T₂ imaging for high-precision gel dosimetry: III. Effects of temperature drift during scanning. *Phys. Med. Biol.*, **46**: 2697-2711.
9. De Deene Y, Reynaert N, De Wagter C (2001) On the accuracy of monomer/polymer gel dosimetry in the proximity of a high-dose-rate Ir-192 source. *Physics in Medicine and Biology*, **46**: 2801-2825.
10. Gustavsson H (2004) Radiotherapy gel dosimetry, development and application of normoxic polymer gels. [Ph.D Thesis], Malmo University Hospital, Lund University, Lund, Sweden.
11. Watanabe Y (2006) 3D dosimetry with polymer gel. In: MN- NCCAAPM Meeting; 2006 April 28; Minneapolis.
12. De Deene Y, Van de Walle R, Achten E, De Wagter C (1998) Mathematical analysis and experimental investigation of noise in quantitative magnetic resonance imaging applied in polymer gel dosimetry. *Signal Processing*, **70**: 85-101.
13. Baldock C, Lepage M, Back SA, Murry PJ, Jayasekera PM, Porter D, et al. (2001) Dose resolution in radiotherapy gel dosimetry: effect of echo spacing in MRI pulse sequence. *Physics in Medicine and Biology*, **46**: 449-460.
14. Westbrook C, Kaut C (1993) MRI in practice. First edition, Blackwell Scientific Publication, London, Oxford, UK.
15. De Deene Y (2004) Fundamentals of MRI measurements for gel dosimetry. *Journal of Physics*, **3**: 87-114.